Biomaterials Science

ROYAL SOCIETY OF CHEMISTRY

PAPER

View Article Online
View Journal | View Issue

Cite this: *Biomater. Sci.*, 2024, **12**, 2312

Enhanced ROS scavenging and tissue adhesive abilities in injectable hydrogels by protein modification with oligoethyleneimine†

Debabrata Palai, [a] Miho Ohta,[a] Iga Cetnar,[a,b] Tetsushi Taguchi *[a] and Akihiro Nishiguchi *[a]

Postsurgical treatment comprehensively benefits from the application of tissue-adhesive injectable hydrogels, which reduce postoperative complications by promoting wound closure and tissue regeneration. Although various hydrogels have been employed as clinical tissue adhesives, many exhibit deficiencies in adhesive strength under wet conditions or in immunomodulatory functions. Herein, we report the development of reactive oxygen species (ROS) scavenging and tissue-adhesive injectable hydrogels composed of polyamine-modified gelatin crosslinked with the 4-arm poly (ethylene glycol) crosslinker. Polyamine-modified gelatin was particularly potent in suppressing the secretion of proinflammatory cytokines from stimulated primary macrophages. This effect is attributed to its ability to scavenge ROS and inhibit the nuclear translocation of nuclear factor kappa-B. Polyamine-modified gelatin-based hydrogels exhibited ROS scavenging abilities and enhanced tissue adhesive strength on collagen casing. Notably, the hydrogel demonstrated exceptional tissue adhesive properties in a wet environment, as evidenced by its performance using porcine small intestine tissue. This approach holds significant promise for designing immunomodulatory hydrogels with superior tissue adhesion strength compared to conventional medical materials, thereby contributing to advancements in minimally invasive surgical techniques.

Received 20th December 2023,
Accepted 11th March 2024

DOI: 10.1039/d3bm02065g

rsc.li/biomaterials-science

Introduction

Injectable hydrogels have been used as medical tissue adhesives for effective wound closure, bleeding control, and tissue sealing, thereby contributing to the prevention of postoperative complications.[1–3] Although conventional treatments using sutures and staples have been applied to tissue damage in surgery and traumatic injury, these methods have certain limitations in blood leakage by suture failure, possibility of bacterial infection, and difficulty in the treatment of soft tissues.[4] In addition, sutures and staples do not possess biological functionalities to control the tissue response during the wound healing process. Injectable hydrogels could be advantageous for critical treatments by alleviating the risk of damaging delicate tissues and providing greater control over wound healing processes.[5,6] As biological tissue is a wet and soft material with layers of interfacial water, which require extra effort to anchor adhesive materials[7,8] various approaches, including chemical reaction-based anchoring and physical interactions (hydrophobic interaction,[9–12] van der Waals force,[13] and hydrogen bonding[14,15]) offer means to enhance adhesion strength without compromising biocompatibility.

Immunomodulation is a critical concept in the realm of biomaterials, which depicts a material's capacity to interface with living entities while mitigating adverse effects, such as injury, toxicity, or rejection by the host's immune system.[16] In the acute phase, the inflammatory response retaliates against pathogens and fungal infections as per the in-body defense mechanism. During the inflammatory phase, pro-inflammatory cytokines are secreted by immune cells, inducing the production of reactive oxygen species (ROS), such as hydrogen peroxide (H_2O_2), hydroxyl radicals, and superoxide anion radicals. Although ROS is a necessary mediator for tissue regeneration, excessive ROS generation often overwhelms native antioxidant activities and nourishes inflammatory responses[17,18] leading to delayed wound healing. To date, tissue-adhesive injectable hydrogels, such as fibrin glue[19,20] and cyanoacrylates,[21,22] have been used clinically, and ROS-scavenging hydrogels[23] have been studied; however, it is still challenging to develop injectable hydrogels with both sufficient tissue

[a]*Research Center for Macromolecules and Biomaterials, National Institute for Materials Science, Namiki 1-1, Tsukuba, Ibaraki 305-0044, Japan. E-mail: nishiguchi.akihiro@nims.go.jp, taguchi.tetsushi@nims.go.jp*
[b]*Faculty of Materials Science and Engineering, Warsaw University of Technology, Al. Waszyngtona 4/8 Warsaw, Poland*

† Electronic supplementary information (ESI) available. See DOI: https://doi.org/10.1039/d3bm02065g

adhesiveness and ROS scavenging toward immunomodulatory functions to facilitate wound healing.

To functionalize the injectable hydrogels, we focused on polyamines that possess multiple amino groups. Biogenic polyamines, including spermine and spermidine, play crucial roles in cellular proliferation, differentiation, and signalling in cytosol.[24] While the precise functions of polyamines remain only partially understood, they exhibit anti-inflammatory properties, including suppression of excessive ROS generation, inhibition of pro-inflammatory cytokines, prevention of neutrophil translocation, and inhibition of macrophage formation.[25–28] We have previously reported that branched oligoethyleneimine (bOEI) possesses anti-inflammatory function *via* ROS scavenging and bOEI-modified hyaluronic acid recovered ulcerative colitis in mice.[29,30] While synthetic polyamines are extensively used to treat inflammatory diseases, the development of a tissue-adhesive hydrogel incorporating anti-inflammatory synthetic polyamines with precisely tuned mechanical strength has not been reported.

In this study, we fabricated a bOEI-modified gelatin-based injectable hydrogel cross-linked with *N*-hydroxy succinimide (NHS)-terminated 4-arm poly(ethylene glycol) (4-arm PEG-NHS) (Fig. 1). Under physiological pH conditions, bOEI is expected to provide excess amino groups, facilitating rapid cross-linking with the 4-arm PEG-NHS. We studied the effects of cross-linking between bOEI and different concentrations of PEG-NHS on the mechanical and adhesive properties of the gel in comparison with those of the collagen casing (membrane). This synthetic hydrogel, with a large number of primary amine groups from polyamines, has the potential to suppress macrophage activation by scavenging excess ROS. The findings of this study may contribute to the design of ROS-scavenging and highly tissue-adhesive injectable hydrogels, enabling minimally invasive surgery and preventing post-operative complications.

Experimental section

Materials

Porcine skin-derived G was purchased from Nitta Gelatin (Tokyo, Japan). bOEI (M_w = 300 and 600 Da) was purchased from Junsei Chemical Co., Ltd (Japan). NHS-terminated 4-arm PEG (M_w = 20 000 Da) was purchased from NOF Corporation (Japan). 1-Ethyl-3-(3-dimethylaminopropyl) carbodiimide hydrochloride (EDC), WST-8 cell counting kit, and 4′6-diamidino-2-phenylindole dihydrochloride (DAPI) were purchased from DOJINDO (Japan). NHS and phosphate buffered saline (PBS) were purchased from Nacalai Tesque (Kyoto, Japan). Enzyme linked immunosorbent assay (ELISA) for mouse TNF-α was purchased from R&D systems (USA). 2-(*N*-Morpholino) ethanesulfonic acid (MES), RPMI 1640 (R8758), fetal bovine serum (FBS), and phalloidin with rhodamine were purchased from Sigma-Aldrich (USA). 2′,7′-Dichlorodihydrofluorescin diacetate (DCF-DA, OxiSelect) was purchased from Cell Biolabs, Inc. (USA). Lipopolysaccharide (LPS, *E. coli*) and paraformaldehyde (PFA) were purchased from Fujifilm Wako Pure Chemical Corporation (Japan). Dialysis membranes (molecular weight cut-off value: 12 000–14 000) were purchased from Repligen (USA). The mouse macrophage colony-stimulating factor (M-CSF) was purchased from Mitenyi Biotec (Munich, Germany). NF-κB p65 antibody (F-6) was purchased from Cell Signaling Technology (USA). The mouse fibroblast cell line (L929) was purchased from RIKEN (Wako, Japan).

Synthesis of GbOEI polymer

To synthesis GbOEI-2, 1 wt% of G was dissolved in 100 mL of 0.1 M MES buffer (pH = 4.8) for 1 h at 50 °C. bOEI (M_w = 300 Da, 3.7 mg) was dispersed in 1 mL of buffer and slowly added to the solution. EDC (238 mg, 1.24 mmol) and NHS (143 mg, 1.24 mmol) were added to the solution and stirred for 24 h at 50 °C. Finally, GbOEI-2 was obtained after dialysis and freeze-drying the sample for 3 d. The number of amino groups in GbOEI was estimated using the 2,4,6,-trinitrobenzensulfonic acid assay. To synthesize the different types of GbOEIs, different feeding ratios of bOEI, EDC, and NHS equivalents to the carboxyl groups were used.

Preparation of BMDMs

All mouse experiments were approved by the Animal Care and Use Committee of the National Institute for Materials Science (no. 58-2019-2). The detailed procedure for BMDM cell preparation is described elsewhere.[29] In brief, mice (female, C57BL/6J, 7-week-old) were euthanized, and the femur and tibia were collected and cleaned with 70% ethanol for 1 min. Bones were washed with RPMI 1640 medium (supplemented with 10% FBS and 1% P/S), and bone marrow cells were collected by flushing the medium using a 25-gauge syringe. After filtration through a 70 μm filter and hemolysis with ACK lysing buffer, cells were collected *via* centrifugation at 1300 rpm for 5 min, washed, and resuspended in differentiation medium (RPMI1640 medium with 10% FBS, 1% P/S, and 40 ng mL^{-1} of M-CSF). Cells were cultured for 5 d at 37 °C in a 5% CO_2 incubator, and differentiated cells were harvested using a scraper for further experiments.

Cell viability assay

BMDM (3×10^4 cells per well) cells, and L929 cells (1×10^4) were seeded in a 96-well cell culture plate and cultured in differentiation medium at 37 °C in an incubator with 5% CO_2 for 24 h. The differentiation medium containing GbOEIs (100 μg mL^{-1}) and LPS (100 ng mL^{-1}) were then added to the cells and incubated for 24 h. Cell morphology was monitored using an optical microscope (EVOS XL Cell Imaging System, Thermo Fisher Scientific, USA) during the incubation. A cell counting kit (WST-8 assay; DOJINDO, Japan) was used to count the number of cells. Briefly, 10 μL of WST-8 reagent was added to each well and incubated for 2 h. Absorbance at 450 nm was recorded using a microplate reader. Cell numbers were calculated using a standard curve.

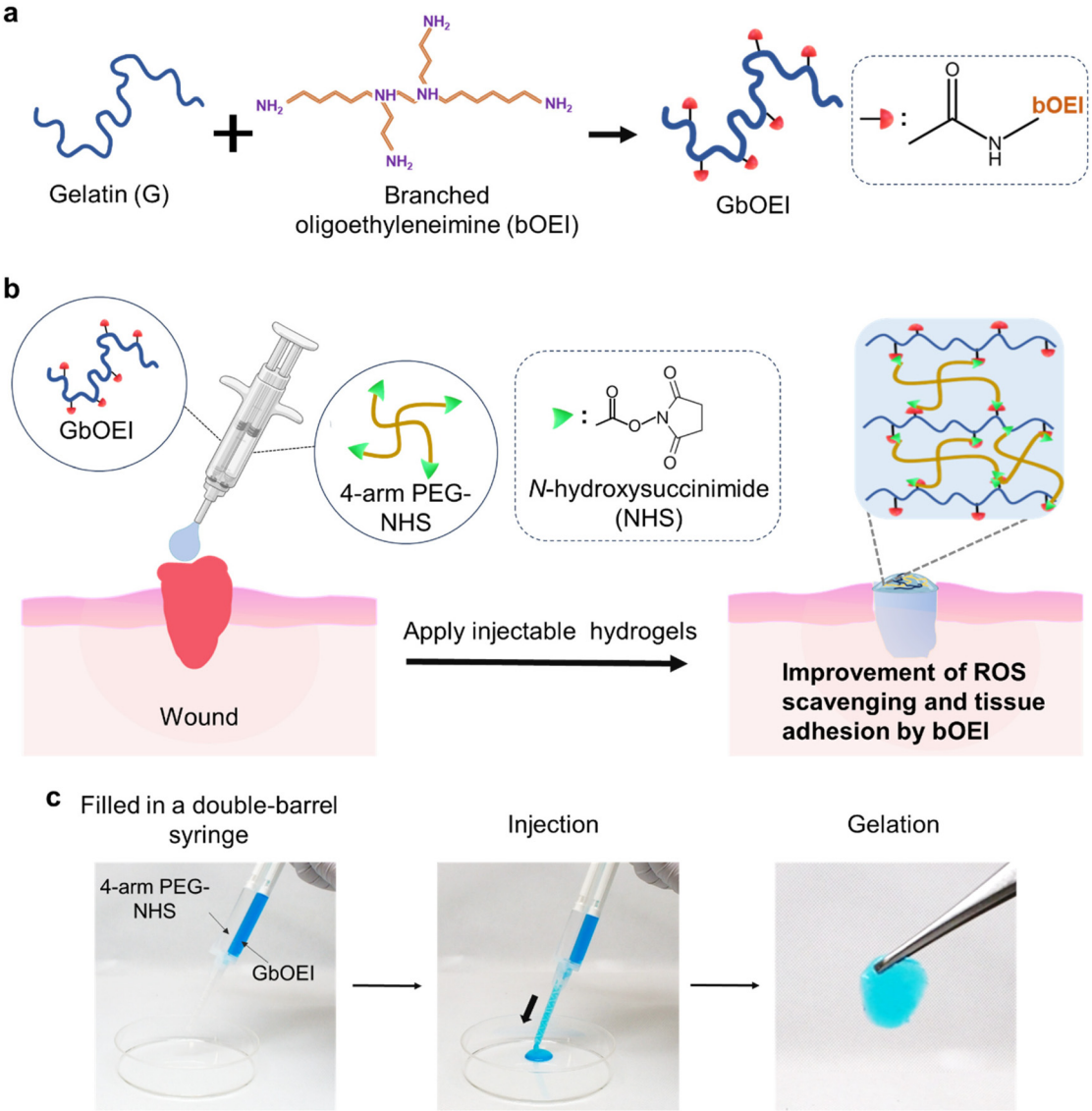

Fig. 1 Schematic presentation of the preparation of branched oligoethyleneimine-modified gelatin (GbOEI)-based tissue adhesive and their application. (a) Synthesis of GbOEI. (b) Schematic of crosslinking between GbOEI and 4-arm PEG-NHS, where ROS scavenging and tissue adhesive abilities of injectable hydrogel were improved by bOEI modification. (c) Demonstration of injectability of the hydrogel using a double barrel spiral needle. Acid blue was used for the visualization of hydrogels.

ELISA

Inflammatory cytokines were quantified using an ELISA kit according to the manufacturer's protocol. BMDM (3×10^4 cells per well) cells were seeded in a 96-well cell culture plate and cultured in the differentiation medium for 24 h. Differentiation medium containing GbOEI samples (100 μg mL^{-1}) and LPS (100 ng mL^{-1}) was added to the cells and incubated for another 24 h. To measure the inflammatory responses of BMDMs, the supernatants were collected carefully and stored in a −80 °C freezer until use. The secretion of tumor necrosis factor-α (TNF-α) from BMDMs was quantified using an ELISA kit. The absorbance at 450 nm was recorded using a microplate reader, and the concentrations were calculated from the standard curve.

Immunofluorescence staining

For immunofluorescence staining, BMDMs were cultured on glass-bottom chamber slides (Matsunami, Japan) in a differentiation medium and incubated at 37 °C in an incubator with 5% CO_2. The differentiation medium with or without LPS (100 μg mL^{-1}) and media containing G, GbOEI samples with LPS (100 μg mL^{-1}) were added to the cells and incubated for another 24 h. The cells were fixed using 4% PFA and permeabilized with 0.2% Triton-X for 15 min. After washing with PBS thrice, the cells were blocked with 5% BSA/PBS for 1 h. The cells were then stained using phalloidin with rhodamine and incubated for 1 h at 25 °C, to visualize the actin filaments. The cells were further incubated with anti-mouse NF-κB antibody (1 : 100) for 16 h at 4 °C, followed by incubation with a second-

ary antibody (1 : 500) for 1 h. After washing with PBS, the nuclei were stained with DAPI. Samples were observed using a confocal laser scanning microscope (CLSM; ZEISS LSM 900, Germany).

ROS scavenging assay

ROS scavenging test of gelatin and the hydrogel was performed using the fluorescent probe DCF-DA, which is highly sensitive to hydroxyl radicals. DCF-DA was dissolved in ethanol and diluted with PBS. To assess ROS scavenging of polymer, DCF-DA solution was added to PBS containing G and GbOEI (100 μg mL^{-1}), and H_2O_2 was added then in a light protective 96-well plate. For the hydrogels, pre-gel solution (50 μL) was added to 96-well plate and incubated for 1 h to complete the gelation. H_2O_2 (50 μL) was then added to the gels followed by incubation for 1 h, and DCF-DA (50 μL) was added. The final concentrations of DCF-DA and H_2O_2 were 50 μM and 100 μM, respectively. Consequently, both the gelatin solution and hydrogels were incubated at 37 °C for 1 h, and fluorescence intensity with (excitation wavelength 485 nm and emission wavelength 525 nm) was measured using a microplate reader (Spark10M, TECAN, Switzerland).

Rheological measurement

Rheological measurements were performed using a rheometer (MCR301, Anton Paar GmbH, Austria). G and GbOEI-1, -2, -3, -4 were dissolved in PBS at 10 wt% at 50 °C and kept at 37 °C in a dry bath until the use. 4-arm PEG-NHS crosslinker was dissolved in PBS (10, 20, and 30 wt%) at room temperature. Gelatin and PEG-NHS crosslinkers were mixed and placed on the stage of the rheometer (pre-warmed at 37 °C) using a pipettor, and a jig with a diameter of 10 mm was set at a gap of 1 mm. After removing the excess sample, the time-dependent shear modulus was measured at an angular frequency of 10 rad s^{-1} with 1% shear strain in oscillatory mode. Hydrogel formation through crosslinking was conformed from the point when both the curve of storage modulus (G') and loss modulus (G'') reached plateau.

Tensile test

Tensile strengths were measured using a tensile tester instrument (EZ-S 500 N, Shimadzu, Kyoto, Japan). A mixture of GbOEI or G and PEG crosslinker were poured into a dumbbell-shaped silicone mold (total length 35 mm, width 2 mm and thickness 1 mm, respectively). After the incubation at 37 °C for 30 min in sealed condition, the gels were removed slowly from the mold and fixed with a 1N clamp. The initial distance between the clamps was 20 mm. Tensile tests were performed at a speed of 100 mm min^{-1} as per previous report.[31]

Viscosity measurement

G and GbOEI-2 (100 mg mL^{-1}) were dissolved in PBS at 50 °C. Each sample (2 mL) was placed in a plastic tube and incubated at 37 °C for 20 min. The viscosity of gelatin was measured using a rotational viscometer (ViscomateVM-100A, SEKONIC, Japan) by dipping the measuring probe into the sample solutions. The probe was thoroughly cleaned with deionized water between the measurements of the two different samples.

Swelling behaviour of hydrogel

The swelling ratio of G gel and GbOEI gels was measured by immersing in PBS at 37 °C. G and GbOEI were dissolved in PBS (10 wt%) at 50 °C. 4-arm PEG-NHS crosslinker was dissolved in PBS (10 wt%, 20 wt%, and 30 wt%) at room temperature. The solutions were mixed, and the pre-gel solutions were poured onto a silicon mold to prepare gel sheets with 1 mm thickness. After incubation at 37 °C for 30 min, each gel sheet was cut into 8 mm diameter shaped disks. The gel disks were immersed in PBS (pH = 7.4) and incubated for 24 h at 37 °C. After incubation, the gels were collected and weighed (W_s). The gels were freeze-dried for another 24 h and their dry weights were measured (W_d). The swelling ratio was calculated as follows:

$$\text{Swelling ratio} = (W_s - W_d)/W_d \quad (1)$$

where W_s and W_d represent the weight of swelled and dried gels, respectively.

Degradation test under physiological conditions

GbOEI-2 (10 wt%) and 4-arm PEG-NHS (30 wt%) were dissolved in PBS at 50 °C the and pH of the solution was adjusted. Three milliliters of the crosslinked solution was added to a silicone mold and a 1 mm thick sheet. Using a punch, 5 mm diameter disk was prepared and submerged in PBS for 24 h at 5 °C in seal condition for swelling. The swollen hydrogels were taken in tubes and 1 mg mL^{-1} of collagenase (120 U mL^{-1}, Nacalai Tesque, Inc., Japan) was added and incubated at 37 °C. After incubation for 1, 4, 8, and 24 h, the supernatants were discarded, and the resulting gels were freeze-dried for 1 d and weighed.

Burst strength measurement

Burst strength measurements of the gel were conducted according to the standard protocol of the American Society (ASTM F2392-04).[32] As a tissue model, collagen casing (Nippi, Tokyo, Japan) was used as the tissue model. To measure burst strength, the collagen casing was cut to a diameter of 30 mm with a 3 mm pinhole. Gelatin and 4-arm PEG-NHS were dissolved as previously described. The effect of different concentrations (10, 20, and 30 wt%) of 4-arm PEG-NHS on the burst strength of the gel was studied. The pre-gel solutions were poured on the collagen casing of 15 mm diameter and 3 mm pinhole, supported with silicone disc (1 mm in thickness and 15 mm of an inner diameter) and incubated at 37 °C for 30 min in sealed condition. The collagen casing with the cross-linked hydrogel was then placed onto the burst strength measurement apparatus, and saline flowed underneath the sample at 2 mL min^{-1}. The maximum pressure at which the hydrogel ruptured, either sidewise or in the middle, was recorded.

Tissue adhesion of hydrogels to small intestine

To evaluate the adhesive properties of the GbOEI-2 hydrogel, *ex vivo* models of the porcine-derived small intestine (Tokyo

Shibaura Zouki, Japan) were used. First, the intestines were cleaned and filled with saline solution. A 3 mm puncture was created at the center of the intestine using a biopsy punch (KAI Medical, Japan), and the intestine was held vertically to ensure leakage of saline from the puncture. The excess water was wiped off and the hydrogel was applied, and the adhesive properties of the hydrogel were ensured by applying pressure.

Results and discussion

Synthesis of GbOEI and their anti-inflammatory functions

To address whether the modification of gelatin with bOEI provides anti-inflammatory properties, we prepared four different GbOEIs with different numbers of amino groups *via* EDC/NHS chemistry (Table 1). To prepare different types of GbOEIs, the ratios of EDC to NHS were varied. The contents of amino groups were in the range 501–926 μmol g^{-1} after the modification, and GbOEI-2 showed a 3.3-fold increase in amino groups compared to non-modified G. The introduction of bOEI into GbOEI-2 was characterized using ^{1}H-NMR (Fig. 2a).

Next, cytotoxicity of GbOEI was evaluated using cell culture models of mouse fibroblast cell line (L929 cells) and mouse primary macrophages (BMDMs). L929 cells were exposed to supernatants obtained from each hydrogel after 24 h of incubation. Live/dead, WST-8, and wound healing assay showed that hydrogels were biocompatible and did not inhibit cellular migration (Fig. S1†). After 24 h of incubation of BMDM cells with the four types of gelatin (GbOEI-1,-2,-3, and -4) solutions, GbOEI-2 showed the highest cell viability and was not significantly different from G (Fig. 2b). In contrast, the GbOEI-3 and -4 samples showed lower cell viability than the others, partially due to intra/intermolecular crosslinking with bOEI and the toxicity of bOEI600. As an Inflammation model, BMDMs get stimulated by LPS which binds to LPS binding protein to form a complex with the myeloid differentiation factors 2 and CD14 connecting to Toll-like receptors (TLRs), leading to the activation of NF-κB pathway and initiating production of pro-inflammatory cytokines such as TNF-α.[33–35] To evaluate anti-inflammatory function of GbOEI, the secretion of TNF-α from LPS-stimulated BMDMs was quantified. ELISA result implies that GbOEI-2 substantially supressed TNF-α secretion to a higher extent in LPS-stimulated BMDMs, without jeopardizing cell viability (Fig. 2c). The secretion of TNF-α per individual cell was the most effectively suppressed by GbOEI-2, highlighting the capacity of GbOEI-2 to mitigate cytokine secretion at the level of individual cells (Fig. 2d). GbOEI-4 demonstrated a comparable ability to suppress cytokine release; however, the decrease in cell viability made it a less favorable choice. To understand the anti-inflammatory mechanisms, we further evaluated the capability of GbOEI-2 to impede the nuclear translocation of NF-κB in LPS-stimulated BMDMs. Although bOEI is a positively charged molecule, a previous report has indicated that it does not induce protein aggregation or LPS inactivation through oppositely charged interactions. Moreover, it exhibited highest anti-inflammatory functions by blocking a broad spectrum of innate immune response and inhibiting the NF-κB/activator protein-1 pathways.[29] CLSM

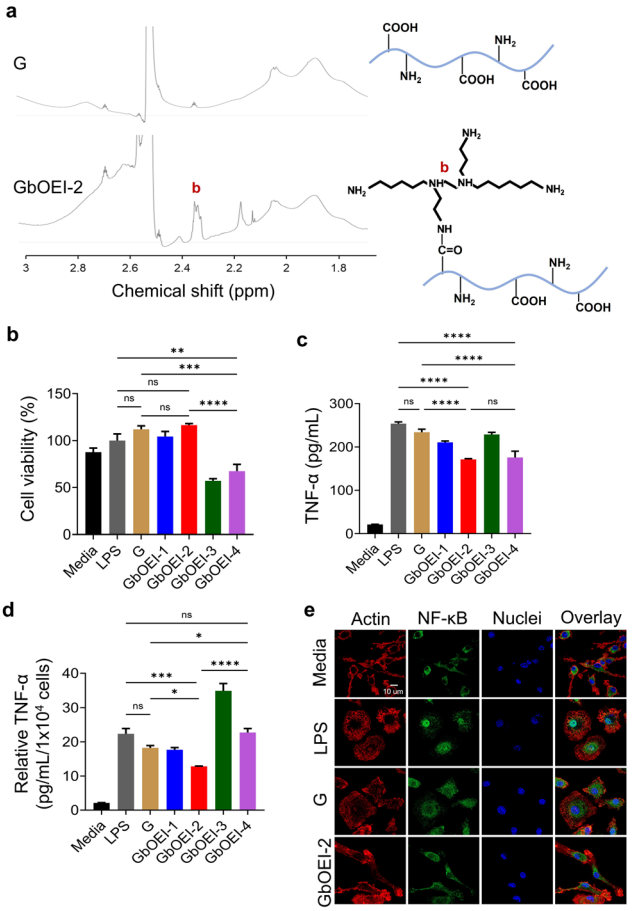

Fig. 2 Anti-inflammatory property of GbOEIs. (a) ^{1}H NMR of G and GbOEI-2 (DMSO, 400 MHz). (b) Cell viability of BMDMs exposed to media, LPS, G and GbOEI solutions (n = 3). (c) The amount of TNF-α secreted from LPS-stimulated BMDMs in the presence of G and GbOEI (n = 3). (d) The amount of TNF-α secretion per 1 × 10^4 cells (n = 3). (e) CLSM image of BMDMs exposed to media, LPS, LPS + G, and LPS + GbOEI-2. NF-κB p65 (green) and nuclei (blue) were stained with NF-κB p65 antibody and DAPI, respectively. Data are presented as mean ± s.d. *P < 0.05, **P < 0.01, ***P < 0.001, ****P < 0.0001, analyzed using the one-way ANOVA, followed by Tukey's multiple comparison *post hoc* test. n.s. denotes not significant.

Table 1 Synthesis of gelatin with different amount of amino groups

Gelatin	Molecular weight of bOEI (Da)	Content of amino groups in gelatin (μmol g^{-1})	Ratio of equivalents to carboxyl groups			Yield (%)
			bOEI	EDC	NHS	
G	—	282	—	—	—	97
GbOEI-1	300	501	10	10	1	108
GbOEI-2	300	926	10	1	1	99
GbOEI-3	300	627	1	1	1	72
GbOEI-4	600	721	5	1	1	97

The amino groups in gelatin was calculated by determining the residual amino groups using 2,4,6,-trinitrobenzensulfonic acid (TNBS).

observation also corroborate that GbOEI-2 effectively suppressed the nuclear translocation of NF-κB in LPS-stimulated BMDMs, while localization of NF-κB in nuclei was partially observed in G (Fig. 2e). These results indicate that GbOEI-2 exerts anti-inflammatory effects by suppressing the nuclear translocation of NF-κB, which agrees with our previous finding.[29]

ROS scavenging ability of gelatin and hydrogel

Considering the ROS-scavenging abilities of biogenic polyamines, we postulated that GbOEI might have ROS scavenging ability which contribute in anti-inflammatory effects.[25] Oxidative stress serve a pivotal role in the physiological defense mechanisms of living organisms. However, the overproduction of ROS impedes tissue regeneration in injured tissues and induces adverse effects, such as inflammation, necrosis, and fibrotic scarring.[18] Consequently, biomaterials capable of scavenging excess ROS at the wound site are integral to promoting regeneration by immunomodulation. The ability to scavenge hydroxyl radicals was quantified using DCF-DA, which is ordinarily non-fluorescent but increases fluorescence intensity in response to hydroxyl radicals. In contrast to G, GbOEI-2 and -4 effectively reduced hydroxyl radicals generated by H_2O_2, functioning as ROS scavengers (Fig. 3a). In agreement with the spermine-mediated ROS scavenging mechanism, the quantity of primary amines present in GbOEI plays a crucial role.[25] Moreover, in the GbOEI hydrogel, the primary amine was consumed during the crosslinking reaction with 4-arm PEG-NHS, but the GbOEI-2 hydrogel still exhibited ROS-scavenging ability (Fig. 3b). Excessive ROS generation triggers the activation of upstream kinases, such as IkB kinase (IKK), leading to the phosphorylation and degradation of the inhibitor protein IkB.[34] This process promotes the nuclear translocation of NF-κB and the transcription of pro-inflammatory genes. Therefore, the ROS-scavenging ability of GbOEI hydrogels may suppress a series of excessive inflammatory responses and function as immunomodulatory biomaterials. In our previous investigation we evidentially proposed a mechanism of bOEI sample where it supress inflammatory responses by scavenging excessive intracellular or extracellular ROS and inhibiting the nuclear translocation of NF-κB.[29] It also supports the ROS scavenging ability and anti-inflammatory functions of GbOEI hydrogels.

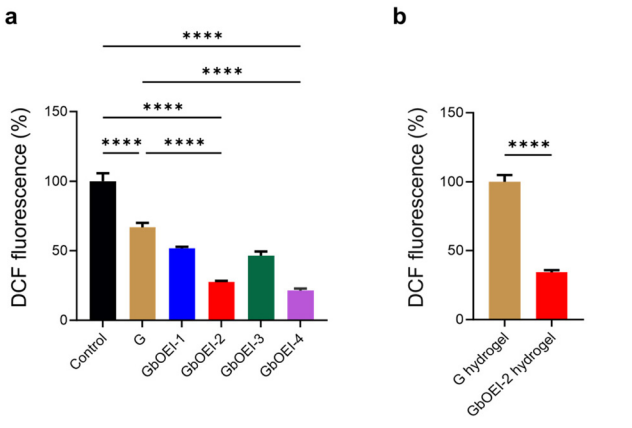

Fig. 3 ROS scavenging property. (a) ROS scavenging of G, GbOEI-1, -2, -3, -4 (n = 3). DCF fluorescence of control was set to 100%. (b) ROS scavenging of G hydrogel crosslinked with 10 wt% 4-arm PEG-NHS and GbOEI-2 hydrogel crosslinked with 30 wt% 4-arm PEG-NHS. DCF fluorescence of G hydrogel was set to 100%. Data are presented as mean ± s.d. ****P < 0.0001, analyzed using the one-way ANOVA, followed by Tukey's multiple comparison *post hoc* test for (a) and Student's t-test for (b).

Mechanical property of GbOEI hydrogels and injectibility

PEG is a biocompatible polymer widely used to formulate tissue-adhesive materials.[36,37] As 4-arm PEG-NHS has high reactivity towards nucleophilic amino groups, the increase in amino groups in gelatin may trigger rapid gelation by increasing the crosslinking points. It is expected that the crosslinked hydrogel will strongly adhere to tissues through a reaction between the remaining NHS groups and the primary amines of proteins in the tissue.[38] For efficient crosslinking, depending on the number of amino groups in G and GbOEI, the concentrations of 4 arm PEG-NHS can be varied. In the case of the unmodified G hydrogel, a high elastic modulus and loss modulus were achieved at 10 wt% concentration of the 4-arm PEG-NHS (Fig. 4a and b). In contrast, the highest elastic and loss moduli for the GbOEI-2 hydrogel were achieved with 30 wt% 4-arm PEG-NHS. Nevertheless, the storage modulus of the GbOEI-2 hydrogel reached a plateau within a few minutes, which was sufficient to meet the time required for clinical mixing and injection of the gel.[39] Mechanical strength of GbOEI-2, G hydrogel was evaluated by tensile test. At 25 °C, GbOEI-2 hydrogel exhibited 1.5 fold increase in fracture strain (245%) and 3.6 fold increase in fracture strength (90.4 kPa) compared to G hydrogel (Fig. 4c and d). Furthermore, the swelling ratio of the GbOEI-2 hydrogel was 43, which is a 1.9-fold increase compared with that of the G hydrogel. To understand the injectability at physiological temperature, viscosity of the GbOEI solutions was measured at 37 °C. The viscosities of all GbOEI solutions were substantially lower than those of G (Fig. 4e). This observation supported the injectability of bOEI at physiological temperatures. GbOEI solution was liquid even at room temperature (~25 °C) partly due to chemical structural changes of gelatin by bOEI modification and there was no need to warm up when used. The biodegradability of hydrogels was evaluated using collagenase (Fig. 4f). During the incubation of the GbOEI-2 hydrogels in the presence of collagenase, the weight gradually decreased, indicating that the hydrogels were enzymatically degradable.

Tissue adhesive property of hydrogel

Various hydrogel was developed using multiple hydrogen and ionic bonds for wearable devices, and human–machine interfaces but tough tissue adhesive hydrogel synthesized using conjugation reaction between highly reactive primary amine and 4-arm PEG-NHS can be advantageous for minimally invasive surgery.[40] The tissue adhesive properties of the GbOEI hydrogels were determined according to the ASTM standard protocol with the instrumental setup (Fig. 5a). To conduct the test with maximal efficacy, the hydrogel needs to effectively

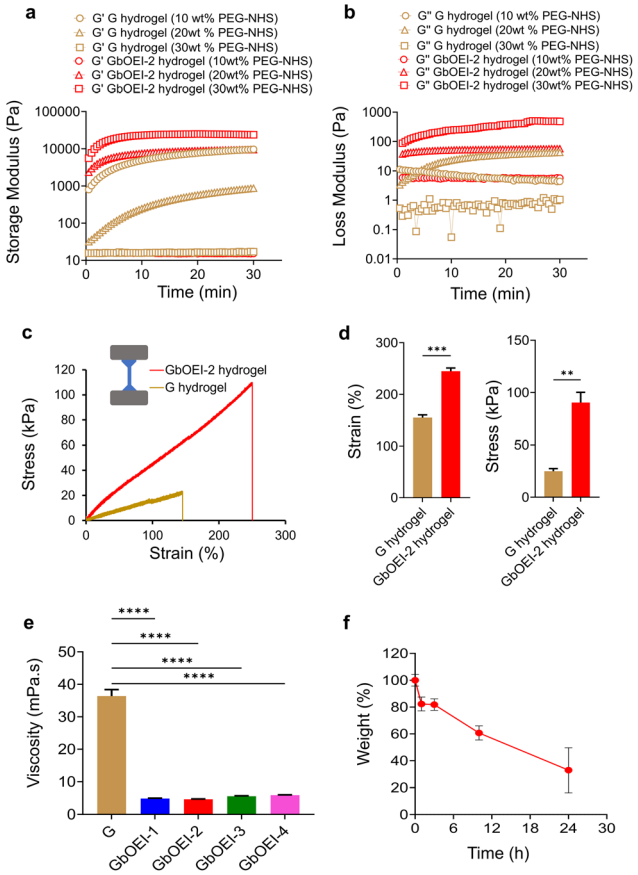

Fig. 4 Rheological property and biodegradability of hydrogels. (a and b) Rheological analysis of G and GbOEI-2 crosslinked with different concentration of 4-arm PEG-NHS. Time-dependent storage modulus (*G'*) and loss modulus (*G''*) were measured at an angular frequency of 10 rad s^{-1} with 1% shear strain in an oscillatory mode at 37 °C. (c) Tensile test of G and GbOEI-2 hydrogels. (d) The fracture strain and stress exhibited by G and GbOEI-2 gel (n = 3). The measurement was performed at 25 °C. (e) The viscosity of gelatin solutions at 37 °C. (f) Biodegradability test of GbOEI-2 hydrogels using collagenase under physiological conditions. Data are presented as mean ± s.d. $^{**}P < 0.01$, $^{***}P < 0.001$, $^{****}P < 0.0001$, analyzed using the one-way ANOVA, followed by Tukey's multiple comparison *post hoc* test.

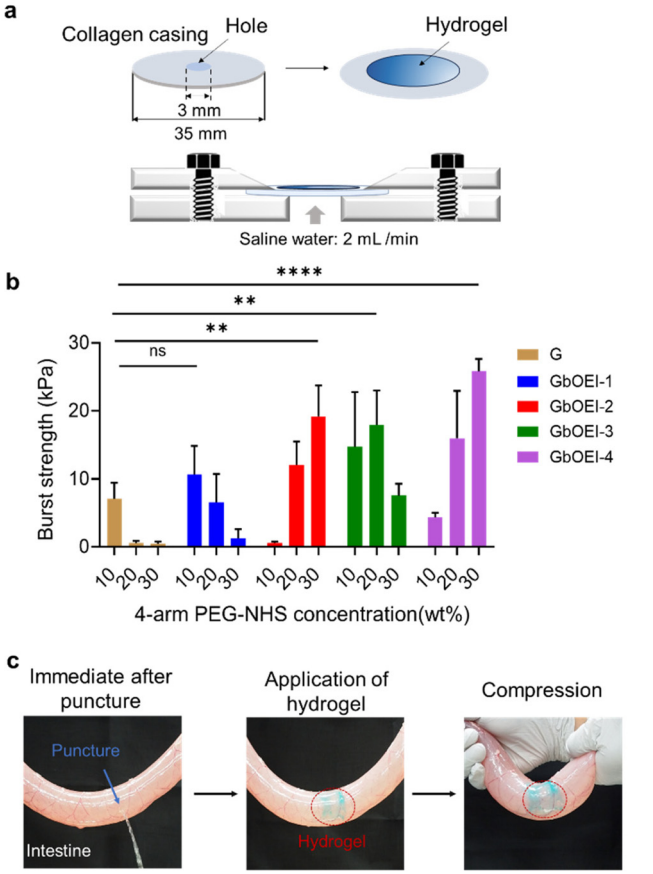

Fig. 5 Tissue adhesive property of hydrogels. (a) Schematic of burst pressure measurement. (b) Burst pressure of hydrogels of G and GbOEI-1, -2, -3, -4 crosslinked with 4-arm PEG-NHS (n = 3). (c) Images of the adhesion test using small intestine of porcine. Acid blue was used for the visualization of hydrogels. Data are presented as mean ± s.d. $^{**}P < 0.01$ and $^{****}P < 0.0001$, analyzed using one-way ANOVA, followed by Tukey's multiple comparison *post hoc* test. n.s. denotes not significant.

interface with the underlying collagen casing and manifest mechanical strength that surpasses the physiological loading conditions. Burst-strength measurements were performed to quantify the adhesive capability of the hydrogel under increasing liquid pressure. Sustaining the maximum pressure until rupture signifies the mechanical resilience of the hydrogel. The results indicated that the GbOEI-2 and -4 hydrogels crosslinked with 30 wt% 4-arm PEG-NHS demonstrated the highest burst strength and exhibited an increase of more than two-fold compared to that of the G hydrogel (Fig. 5b). For GbOEI-1, -3, optimal strength was attained when these gelatins were crosslinked with 10 wt% and 20 wt% 4-arm PEG-NHS, respectively. Modification with bOEI enhanced the burst strength partly because of the improved mechanical strength and anchoring with proteins in the tissues. However, GbOEI hydrogels crosslinked with 30 wt% 4-arm PEG-NHS exhibited better adhesion strength and anti-inflammatory properties compared with commercially available and other reported adhesives (Table S1†). The sealing properties of the hydrogel were investigated using the porcine small intestine. Immediately after the puncture, saline water started draining from the puncture site. After applying the GbOEI-2 hydrogel to the puncture site, the intestine was refilled with saline water, but the draining of the saline water was stopped immediately (Fig. 5c). Even when pressure was applied to the puncture site, the GbOEI-2 hydrogel firmly sealed the puncture, indicating that GbOEI hydrogels can be used to treat wounds under wet conditions to prevent postoperative complications.

Conclusion

In conclusion, we developed ROS scavenging and tough tissue adhesives achieved through the modification of gelatin with cationic bOEI. Upon comparing various Gs containing different compositions of bOEI, it was established that GbOEI-2 exhibited

the highest cytocompatibility and anti-inflammatory and ROS-scavenging abilities. GbOEI-2 effectively suppressed the secretion of inflammatory cytokines in LPS-stimulated BMDMs by ROS scavenging and inhibiting the nuclear translocation of NF-κB. GbOEI-2 hydrogels cross-linked with 4-arm PEG-NHS demonstrated an exceptional capacity to mitigate ROS overproduction. The viscosity of the GbOEI-2 solution at physiological temperatures remained sufficiently low for injectability. The GbOEI-2 hydrogel exhibited remarkable tissue adhesion and sealing properties when applied to collagen casings and porcine-derived intestinal tissue. Our findings may promote scarless wound healing and enhance the quality of minimally invasive surgeries. This innovation has the potential to reduce the postoperative complications and burden.

Conflicts of interest

The authors declare no conflict of interest.

Acknowledgements

We appreciate financial support from the Japan Society for the Promotion of Science (JSPS) KAKENHI (Grant No. 22H03962 and 23H01718) and the Uehara Memorial Foundation.

References

1 B. Petersen, A. Barkun, S. Carpenter, P. Chotiprasidhi, R. Chuttani, W. Silverman, N. Hussain, J. Liu, G. Taitelbaum, G. G. Ginsberg and Technology Assessment Committee, American Society for Gastrointestinal Endoscopy, *Gastrointest. Endosc.*, 2004, **60**, 327–333.
2 N. Lang, M. J. Pereira, Y. Lee, I. Friehs, N. V. Vasilyev, E. N. Feins, K. Ablasser, E. D. O'Cearbhaill, C. Xu, A. Fabozzo, R. Padera, S. Wasserman, F. Freudenthal, L. S. Ferreira, R. Langer, J. M. Karp and P. J. del Nido, *Sci. Transl. Med.*, 2014, **6**, 218ra6.
3 D. M. Sidle, B. M. Loos, A. L. Ramirez, S. S. Kabaker and C. S. Maas, *Arch. Facial Plast. Surg.*, 2005, **7**, 393–397.
4 C. D. Owens and K. Stoessel, *J. Hosp. Infect.*, 2008, **70**, 3–10.
5 L. Yu and J. Ding, *Chem. Soc. Rev.*, 2008, **37**, 1473–1481.
6 H. J. Chung and T. G. Park, *Nano Today*, 2009, **4**, 429–437.
7 M. Tanaka, T. Hayashi and S. Morita, *Polym. J.*, 2013, **45**, 701–710.
8 E. A. Q. Mondarte, E. M. M. Zamarripa, R. Chang, F. Wang, S. Song, H. Tahara and T. Hayashi, *Langmuir*, 2022, **38**, 1324–1333.
9 A. Nishiguchi, F. Sasaki, H. Maeda, M. Kabayama, A. Ido and T. Taguchi, *Small*, 2019, **15**, e1901566.
10 Y. Mizuno, R. Mizuta, M. Hashizume and T. Taguchi, *Biomater. Sci.*, 2017, **5**, 982–989.
11 D. Palai, H. Tahara, S. Chikami, G. V. Latag, S. Maeda, C. Komura, H. Kurioka and T. Hayashi, *ACS Biomater. Sci. Eng.*, 2022, **8**, 3765–3772.
12 G. V. Latag, T. Nakamura, D. Palai, E. A. Q. Mondarte and T. Hayashi, *ACS Appl. Bio Mater.*, 2023, **6**, 1185–1194.
13 S. Rose, A. Prevoteau, P. Elzière, D. Hourdet, A. Marcellan and L. Leibler, *Nature*, 2014, **505**, 382–385.
14 H. Lee, B. P. Lee and P. B. Messersmith, *Nature*, 2007, **448**, 338–341.
15 E. A. Q. Mondarte, J. Wang and J. Yu, *ACS Biomater. Sci. Eng.*, 2023, **9**, 5679–5686.
16 L. Ghasemi-Mobarakeh, D. Kolahreez, S. Ramakrishna and D. Williams, *Curr. Opin. Biomed. Eng.*, 2019, **10**, 45–50.
17 H. Wu, F. Li, W. Shao, J. Gao and D. Ling, *ACS Cent. Sci.*, 2019, **5**, 477–485.
18 M. Cano Sanchez, S. Lancel, E. Boulanger and R. Neviere, *Antioxidants*, 2018, **7**, 98.
19 W. D. Spotnitz, *ISRN Surg.*, 2014, **2014**, 1–28.
20 M. Radosevich, H. A. Goubran and T. Burnouf, *Vox Sang.*, 1997, **72**, 133–143.
21 F. Leonard, R. K. Kulkarni, J. Nelson and G. Brandes, *J. Biomed. Mater. Res.*, 1967, **1**, 3–9.
22 P. A. Leggat, D. R. Smith and U. Kedjarune, *ANZ J. Surg.*, 2007, **77**, 209–213.
23 H. Nakagawa, Y. Matsumoto, Y. Matsumoto, Y. Miwa and Y. Nagasaki, *Biomaterials*, 2015, **69**, 165–173.
24 C. L. A. N. Seiler, in *Progress in Drug Research/Fortschritte der Arzneimittelforschung/Progrès des recherches pharmaceutiques*, Birkhäuser Basel, Basel, 1994, vol. 42.
25 H. C. Ha, N. S. Sirisoma, P. Kuppusamy, J. L. Zweier, P. M. Woster and R. A. Casero Jr., *Proc. Natl. Acad. Sci. U. S. A.*, 1998, **95**, 11140–11145.
26 M. Zhang, T. Caragine, H. Wang, P. S. Cohen, G. Botchkina, K. Soda, M. Bianchi, P. Ulrich, A. Cerami, B. Sherry and K. J. Tracey, *J. Exp. Med.*, 1997, **185**, 1759–1768.
27 A. Ferrante, *Immunology*, 1985, **54**, 785–790.
28 Y. L. Latour, A. P. Gobert and K. T. Wilson, *Amino Acids*, 2020, **52**, 151–160.
29 A. Nishiguchi and T. Taguchi, *Adv. Funct. Mater.*, 2021, **31**, 2100548.
30 A. Nishiguchi and T. Taguchi, *J. Mater. Chem. B*, 2023, **11**, 4005–4013.
31 A. Nishiguchi, S. Ito, K. Nagasaka, H. Komatsu, K. Uto and T. Taguchi, *Biomaterials*, 2024, **305**, 122451.
32 Astm F-04, *Standard test method for burst strength of surgical sealants*, ASTM International, West Conshohocken, PA, 2015.
33 S. Akira and K. Takeda, *Nat. Rev. Immunol.*, 2004, **4**, 499–511.
34 M. J. Morgan and Z.-G. Liu, *Cell Res.*, 2011, **21**, 103–115.
35 Q. Li and I. M. Verma, *Nat. Rev. Immunol.*, 2002, **2**, 725–734.
36 A. Nishiguchi and T. Taguchi, *ACS Appl. Bio Mater.*, 2020, **3**, 9093–9100.
37 E. W. Merrill and E. W. Salzman, *ASAIO J.*, 1983, **6**, 60–64.
38 H. Tan, D. Jin, X. Qu, H. Liu, X. Chen, M. Yin and C. Liu, *Biomaterials*, 2019, **192**, 392–404.

39 I. Kim, J. S. Choi, S. Lee, H. J. Byeon, E. S. Lee, B. S. Shin, H.-G. Choi, K. C. Lee and Y. S. Youn, *J. Controlled Release*, 2015, **214**, 30–39.

40 D. Zhang, F. Yang, J. He, L. Xu, T. Wang, Z.-Q. Feng, Y. Chang, X. Gong, G. Zhang and J. Zheng, *ACS Appl. Polym. Mater.*, 2020, **2**, 1031–1042.